Chem Biol Drug Des 2015; **86:** 626–636

Research Article

Novel Diketopiperazine Dihydroorotate Dehydrogenase Inhibitors Purified from Traditional Tibetan Animal Medicine Osteon Myospalacem Baileyi

Lei Jiang[1,2,†], Huaixiu Wen[1,2,†], Yun Shao[1], Ruitao Yu[1], Zenggen Liu[1], Shuo Wang[1,2], Qilan Wang[1], Xiaohui Zhao[1], Peng Zhang[3], Yanduo Tao[1,*] and Lijuan Mei[1,*]

[1]*Key Laboratory of Tibetan Medicine Research, Northwest Plateau Institute of Biology, Chinese Academy of Sciences, Xining 810001, China*
[2]*University of Chinese Academy of Sciences, Beijing 100039, China*
[3]*University of Electronic Science and Technology of China, Chengdu 611731, China*
**Corresponding authors: Yanduo Tao and Lijuan Mei, Chrisjiang27@Gmail.com*
The corresponding authors share the E-mail address and Telephone number.
[†]Contributing equally to the work.

Traditional Tibetan medicine provides an abundant source of knowledge on human ailments and their treatment. As such, it is necessary to explore their active single compounds used to treat these ailments to discover lead compounds with good pharmacologic properties. In this present work, animal medicine, Osteon Myospalacem Baileyi extracts have been separated using a two-dimensional preparative chromatographic method to obtain single compounds with high purity as part of the following pharmacological research. Five high-purity cyclic dipeptides from chromatography work were studied for their dihydroorotate dehydrogenase inhibitory activity on recombinant human dihydroorotate dehydrogenase enzyme and compound Fr. 1-4 was found to contain satisfying inhibition activity. The molecular modeling study suggests that the active compound Fr. 1-4 may have a teriflunomide-like binding mode. Then, the energy decomposition study suggests that the hydrogen bond between Fr. 1-4 and Arg136 can improve the binding mode to indirectly increase the van der Waals binding energy. All the results above together come to the conclusion that the 2, 5-diketopiperazine structure group can interact with the polar residues well in the active pocket using electrostatic power. If some proper hydrophobic groups can be added to the sides of the 2, 5-diketopiperazine group, it is believed that better 2, 5-diketopiperazine dihydroorotate dehydrogenase inhibitors will be found in the future.

Key words: cyclic dipeptides, Dihydroorotate dehydrogenase inhibitors, Osteon Myospalacem Baileyi, Tibetan medicine, two-dimensional chromatography

Received 10 November 2014, revised 15 January 2015 and accepted for publication 19 January 2015

Osteon Myospalacem Baileyi, known as Sai long gu (in Tibetan language, 'blind rat bone'), is the whole skeleton of the Tibetan plateau rodentia animal *Myospalax Baileyi Thomas*. Osteon Myospalacem Baileyi has been widely used in the Tibetan region, and since 1991, Osteon Myospalacem Baileyi has been listed in the Pharmacopoeia of the People's Republic of China as a new first-class animal medical material. The medicinal properties of Osteon Myospalacem Baileyi's crude extract have been proven by modern pharmacological research, including studies on antirheumatoid arthritis (1), anti-osteoporosis (2), analgesics (3), and anti-inflammation (4). However, the complexity of Osteon Myospalacem Baileyi extracts makes purification so difficult that very little information about their chemical composition has been reported, and even less information on the chemical compounds responsible for therapeutic effects. Therefore, it is extremely desirable to separate the single compounds from Osteon Myospalacem Baileyi in order to conduct the following pharmacological research activity.

Preparative HPLC is one of the most efficient technologies used in the preparation of single chemicals in complex samples, which is applied in separating compounds from complex Chinese traditional medicine in recent years. However, taking into account the complex chemical composition of natural medicinal extracts, it is virtually impossible to obtain compounds of high purity by only one-dimensional preparation due to limited resolution and peak capacity. Two-dimensional HPLC separation, associated with enlarged peak capacity and enhanced selectivity, seems to be potentially suitable for the purification of single compounds from complex crude samples (5). In the process of two-dimensional HPLC purification, several chromatographic separation modes can be selected, and different systems can be constructed for the separation of complex matrices with different properties in which RPLC

 doi: 10.1111/cbdd.12530

coupled with reversed-phase liquid chromatography (RP/RP-LC) is one of the most prospective separation systems available owing to its high separation efficiency (6–9). In light of the above, an RP/RP-LC two-dimensional HPLC separation system was employed for the purification of single compounds from a crude sample of Osteon Myospalacem Baileyi in the current work.

Cyclic dipeptides (CDPs) are generated by cyclization of two amino acids, and they characteristically contain a 2, 5-diketopiperazine skeleton. CDPs, commonly biosynthesized from amino acids, are found in various nature products such as cordyceps sinensis (10), cocoa (11), roasted coffee (12), and marine sponge *Axinella vaceleti* (13). Some of the chemical properties of 2, 5-diketopiperazines, such as a resistance to proteolysis, mimicking of peptidic pharmacophoric groups, substituent group stereochemistry (defined and controlled in up to four combinations), conformational rigidity, and donor and acceptor groups for hydrogen bonding (favouring interactions with biological targets), can be very interesting for medicinal chemistry. In addition, the compounds show a common scaffold, which is easily obtained by conventional procedures that favor structural diversity as a function of substituent side chains, particularly orientated. Favorable pharmacodynamic and pharmacokinetic characteristics are acquired by the compounds through these properties, leading to promising agents for the development of new drugs (14–16).

Dihydroorotate dehydrogenase (DHODH), localized in the mitochondria, is an enzyme essential to pyrimidine *de novo* biosynthesis (17). It catalyzes oxidative conversion of dihydroorotate to orotate using the cofactors flavin mononucleotide (FMN) and ubiquinone (CoQ) in the redox process. As blocking pyrimidine biosynthesis has an antiproliferative effect on rapidly dividing cells (18), inhibitors of human DHODH (hDHODH) have been pursued and developed for the treatment of cancer (19,20) and immunologic disorders, such as rheumatoid arthritis (21) and multiple sclerosis (22). Inhibitor of human DHODH has been shown to be the active metabolite of a recently approved treatment for rheumatoid arthritis. Strong evidence has also been reported that the mechanism for action in the positive control of the drug teriflunomide (A771726) is the inhibition of *de novo* pyrimidine biosynthesis in these cells (23,24).

Drug discovery from natural products includes a multidisciplinary approach combining biological science, organic chemistry, and chromatography science. Drug discovery starts with an analysis of binding sites in target proteins, or an identification of structural motifs common to active compounds, and ends with the generation of small molecule 'leads' suitable for further chemical synthetic work. Focal points include, but are not limited to, analysis of protein–ligand complexes (database searching, docking, and *de novo* design), quantitative assessment of binding interactions (free energy calculations and scoring functions), development of pharmacophores, and analog design. Due to rapid advances in structural biology and computer technology, structure-based computer aided drug design (CADD) using docking techniques, virtual screening, and library design, along with target/structure, focusing combinatorial chemistry, has become a powerful tool in new drug discovery (25–27).

In this study, an RP/RP-LC two-dimensional HPLC separation method was used for the preparation of single compounds from a complex sample extracted from Osteon Myospalacem Baileyi. The inhibition capacities of purified single compounds were then tested in a recombinant human DHODH enzymatic assay. At last, we performed a docking study of the purified single compounds against the molecular target DHODH receptor to investigate the interaction of the purified single compounds with the residues present at the active site. As far as we knew, few HPLC column chromatograph purification methods for the separation of mammal organ extracts could be found. The RP/RPLC two-dimensional separation method used for the purification of the compounds in mammal bone extract could serve as a good reference for following similar separation work. Additionally, the results of the DHODH assay could also provide some useful information for the CDPs research, both in functional food or medicinal areas.

Materials and Methods

Apparatus and reagents

A prep-HPLC system was used for the purification of single compounds. The system consisted of two prep-HPLC pumps, an UV detector, and an HPLC workstation (Hanbang, China).

Chromatographic analysis was performed on an Agilent HPLC system which contained an Agilent 1260 Infinity Binary Pump, an Agilent 1260 Infinity Diode Array detector, an Agilent 1260 Standard Degasser, an Agilent 1260 autosampler, an Agilent Infinity Thermostatted Column Compartment, and an Agilent 1260 Infinity HPLC work station software (Agilent, Santa Clara, CA, USA).

MS and NMR were employed for the analysis of chemical structures. Mass spectrometry was performed on a Bruker esquire 6000 LC-MS (Bruker, Karlsruhe, Germany). The NMR spectrum was measured by a Bruker DXR 600 NMR spectrometer (Bruker) with CD_3OD as a solvent.

The solvent of Prep-HPLC grade mobile phase was purchased from Concord Technology Co. Ltd., Tianjin, China.

Dihydroorotate (DHO), CoQ_{10}, 2, 6-dichloroindophenol (DCIP), phenylmethylsulfonyl fluoride (PMSF), Tris, glycerol, and Triton X-100 were purchased from Sigma Chemistry Co. (St. Louis, MO, USA). The recombinant *Homo sapiens*

dihydroorotate dehydrogenase was purchased from Abnova Co. (Taipei City, Taiwan).

The DISCOVERY STUDIO v 2.5 software (Accelrys Inc., San Diego, CA, USA) was used for molecule modeling.

Sample preparation

Osteon Myospalacem Baileyi was collected from Qinghai Province and authenticated by Professor Lijuan Mei, of the Northwest Institute of Plateau Biology under the Chinese Academy of Science. Nine kilograms of the medicinal material were powdered by an ultrafine grinder machine under −40 °C. Then, the superfine powder was extracted by 100 L deionized water at 60 °C for 60 min, three times. After filtration, the decoctions were combined and concentrated by rotary evaporation at 60 °C in a vacuum. The concentrated decoctions were separated by an n-butyl alcohol/water 1:1 v/v liquid–liquid extraction system. Then, the n-butyl alcohol part was dried by rotary evaporation at 60 °C in a vacuum. The n-butyl alcohol part extract was dissolved in a solution of water/methanol 70:30 v/v and kept for 24 h at 4 °C. After centrifugation, the supernatant was filtered through 0.45 μm membranes. The final concentration of the filtered sample solution was 200 mg/mL.

Chromatographic conditions

The first dimensional preparation was performed on a C18 prep column (50 × 250 mm i.d., 10 μm, 120 Å, DAISO). The mobile phase A was water and mobile phase B was methanol. The linear gradient elution steps were as followed: 0–5 min, 18% B; 5–35 min 18–40% B. The flow rate was 80 mL/min. The sample concentration was 200 mg/mL. The injection volume was 4 mL. Chromatography was recorded at 214 nm. Preparation for the first dimensional purification simplified the extraction of the raw materials into fractions.

Each fraction was analyzed on YMC C18 AQ column (4.6 × 250 mm i.d., 10 μm, 100 Å, YMC). The mobile phase A was water and mobile phase B was methanol. The flow rate was 1 mL/min. The injection volume was 10 μL. The Isocratic elution procedure for fraction 1 was 15% B for 30 min, for fraction 2 was 23% B for 30 min. The chromatographic data were collected at 214 nm.

The second dimensional purification was performed on YMC C18 AQ (10 × 250 mm i.d., 10 μm, 100 Å) column. The mobile phase A was water and mobile phase B was methanol. Fractions collected from the first dimensional separation were further separated on C18 AQ column to obtain single compounds. Different isocratic elution conditions were adopted to separate fractions collected from the first dimensional preparation. The isocratic elution procedure for fraction 1 was 15% for 30 min, for fraction 2 was 23% B for 30 min. The sample concentration was 500 mg/mL. The injection volume was 700 μL. The flow rate was 4 mL/min. The chromatographic data were collected at 214 nm.

Purity test of each single compound was performed on YMC C18 AQ column (4.6 × 250 mm, 5 μm, 100 Å, YMC). The mobile phase A was water and mobile phase B was methanol. The flow rate was 1 mL/min. The injection volume was 10 μL. The linear gradient elution procedure for **Fr. 1-4**, **Fr. 1-5**, and **Fr. 1-6** was 10% to 25% B for 30 min, for **Fr. 2-1** and **Fr. 2-2** was 20% to 35% B for 30 min, respectively. Chromatography data were collected at 214 nm.

Structure identification

The structure of the compounds was determined using nuclear magnetic resonance (NMR) spectroscopy equipped with a 2.5-mm microprobe. NMR Spectrometer using CD_3OD was deployed to measure ^1H and ^{13}C and 2D NMR. All spectra were recorded at 23 °C. One-dimensional ^1H and ^{13}C NMR experiments as well as two-dimensional ^1H-^1H correlation spectroscopy (COSY), ^1H-^{13}C heteronuclear multiple bond correlation (HMBC), and ^1H-^{13}C heteronuclear multiple quantum coherence (HMQC) experiments were performed according to Bruker standard pulse sequences. Chemical shifts are reported relative to the solvent peaks. (CD_3OD: ^1H δ 3.30 and ^{13}C δ 49.0).

MS was performed on a Bruker esquire 6000 LC-MS system under the ion scan mode of 100–500 *m/z* range. Optical rotation of the compounds was measured using a Perkin Elmer PL341 polarimeter (PerkinElmer Co., Waltham, MA, USA) at 25 °C in Methanol.

Inhibition of human DHODH activity

Inhibition of human DHODH activity by the compounds tested was assessed in 96-well plates by a DCIP-linked assay (18). Recombinant human DHODH (final enzyme concentration between 20 and 60 nM in the assay well) were incubated at 37 °C in 50 mM Tris–HCl, 0.1% Triton X-100, 1 mM KCN, pH 8.0 with coenzyme Q_{10} (100 μM), and the tested compounds at different concentrations (final DMSO concentration 0.1% v/v). The reaction was initiated by the addition of DHO (500 μM), and the reduction of DCIP (50 μM) was monitored through a decrease in absorbance at 650 nm. The initial rate of the enzymatic reaction in the presence (V) and in the absence (V1) of an inhibitor was measured, and the IC_{50} value was calculated from eqn (1):

$$V = \frac{V1}{\left(1 + \frac{[I]}{IC_{50}}\right)}. \quad (1)$$

Among which [I] was the inhibitor concentration.

Molecular modeling

Chemical properties of the purified dipeptides were calculated by CHEMBIOOFFICE 2010. The three-dimensional structure of the protein was retrieved from a Protein Data Bank (PDB) which was a repository for the processing and distribution of the 3D structure data of large molecules of proteins and nucleic acids. The docking study of the dipeptides with the DHODH receptor (1D3G and 1D3H) was carried out by Libdock of DISCOVERY STUDIO v 2.5 software (Accelrys Inc.). The software allowed us to virtually screen a database of compounds and predict the strongest binders based on various scoring functions. It explored the ways in which the molecules and their receptors bonded together and docked to each other well.

The three-dimensional structures of positive control drugs and purified dipeptides were drawn by DISCOVERY STUDIO v 2.5 software. Hydrogen bonds were added, and the energy was minimized using CHARMM force field in all the compounds. PDB protein 1D3G and 1D3H structures were chosen for the receptors with a good resolution when compared with other structures. The ligands were removed from the protein, and the chemistry of the protein was corrected for the loss of atoms. Crystallographic disorders and unfilled valence atoms were corrected by alternate conformations and valence monitor tools. Following the above steps of preparations, the protein was subjected to energy minimization by the CHARMM force field. The active site of the protein was first identified, and it was defined as the binding site.

The AMBER 11.0 software was used to perform all the MD simulations in this study. The inhibitors were minimized using the DISCOVERY STUDIO v 2.5 software. General Amber force field (GAFF) parameters were assigned to the ligands, while partial charges were calculated using the AM1-BCC method as implemented in the Antechamber suite of AMBER 11.0. The complexes were neutralized by adding 10 sodium counterions and were surrounded by a periodic box of TIP3P water molecules extending up to 10 Å from the solute. First, energy minimizations using a steepest decent method, followed by the conjugate gradient method, were performed for each system. Then, each system was gradually heated from 0 K to 300 K within 30 ps. This was followed by a further 500 ps of equilibration at 300 K carried out to obtain a stable density. Afterward, an unconstrained production phase was initiated and continued for 4 ns in an NPT ensemble at 1 atm and 300 K. During the simulations, the long-range electrostatic interactions were evaluated by the Particle Mesh Ewald (PME) algorithm. The cutoff distance for the long-range van der Waals interaction was set to 8 Å. The SHAKE method was applied to constrain the bond lengths of hydrogen atoms attached to heteroatoms. The time step used for the MD simulations was set to 2.0 fs, and the trajectory files were collected every 1 ps for the subsequent analysis.

The interaction between inhibitor and each residue was computed using the MM/GBSA decomposition process by the mm_pbsa program in AMBER 11.0. The binding interaction of each inhibitor–residue pair includes three energy terms: van der Waals contribution (G_{vdw}), electrostatic contribution (G_{ele}), and solvation contribution ($G_{solvation}$). All energy components were calculated using the 300 snapshots extracted from the MD trajectory from 1.0 to 4.0 ns.

Results and Discussions

First dimensional separation

The first dimensional preparation was performed on a DAISO C18 prep column. The sample loading was 0.8 g per injection. One whole preparation procedure took 65 min, which consisted of 15 min for column balance, 15 min for column washing, and 35 min for preparation. The retention times of the components differed significantly due to the complex composition of the crude sample. It was not enough to adopt a simple isocratic method. Gradient elution was necessary for the first dimensional preparation. Linear gradient offered the best separation performance for the components with different retention times. Finally, elution methods, including 0–5 min for 18% B and 5–35 min for 18% to 40% B, were used for the preparation. Preparation of the total 2.2 g crude sample required seven injections over an 8-h period. The fractions were collected according to UV absorption intensity to reduce the complexity of each fraction as much as possible. The cross in each fraction had been minimized due to good separation repeatability. As shown in Figure S1, two fractions were collected in the first dimensional separation and their amounts by weight ranged from 0.74 g for **Fr. 1** to 0.58 g for **Fr. 2**.

Purification of the single compounds

To purify the compounds effectively, the separation condition was optimized for each fraction. In this method, the condition optimization was performed in an analytical scale. The analytical scale conditions were transformed to preparative scale conditions. It was found that isocratic conditions were enough for the separation of all the fractions, and the application of an isocratic elution method would avoid extra time for reconditioning in gradient elution. The content of methanol was optimized to ensure the retention time of the peaks between 10 and 40 min. After a minor revision of the elution method of the analytical conditions, the separation conditions were easily transformed to a preparative scale, as shown in Figure S3. The analytical chromatograms in Figure S2 showed similar patterns with the preparative chromatograms in Figure S3, which demonstrated the feasibility of the transformation from an analytical scale to a preparative one. In addition, it was noteworthy that heart cutting was used as the

repeated separation strategy to insure the purity of compounds. The preparation chromatograms of **Fr. 1** and **2** are shown in Figure S3.

After isolating **Fr. 1** and **2**, five pure compounds were obtained and dried through rotary evaporation at 60 °C in a vacuum. All in all, compound 1 (**Fr. 1-4**, 14.1 mg), 2 (**Fr. 1-5**, 12.8 mg), 3 (**Fr. 1-6**, 12.6 mg), 4 (**Fr. 2-1**, 22.1 mg), and 5 (**Fr. 2-2**, 19.2 mg) had enough amounts to be characterized by NMR. In consideration of the impurities with quite different retention times, it was not appropriate to conduct the homogeneity test with isocratic elution methods. The methanol content in the mobile phase was not higher than 30% in the second dimensional preparation. Therefore, linear gradient elution methods described in 2.3 were enough for all the possible impurities to be tested. The purity of these compounds checked by HPLC is shown in Figure S4, and the purity of all compounds was more than 98%. The structures of these compounds are shown in Figure 1. The NMR and ESI-MS data are shown in supporting information Files.

Inhibition of DHODH

The purified dipeptides were assessed for their DHODH inhibitory activity on recombination human DHODH. A procedure adapted from the literature was employed (see Experimental) in which oxidation of DHO to ORO was monitored by following the concomitant reduction of the chromophore 2, 6-dichlorophenolindophenol (DCIP). Teriflunomide was taken as reference. The reduction of DCIP was detected by the decrease in absorbance at 650 nm. The results were collected in Table 1. Analysis of Table 1 shows that compounds **Fr. 1-5**, **Fr. 1-6**, **Fr. 2-1**, and **Fr. 2-2** displayed no inhibitory potency at the dose of 50 μM. However, if a hydroxyl group was added to Pro-γ-carbon site of **Fr. 2-2**, the inhibition potency was about 40 times higher (**Fr. 1-4**). Although the inhibition potency of **Fr. 1-4** was still 11 times lower, compared with positive control teriflunomide, its inhibitory potency was already in the nanomolar range (IC_{50} = 0.77 mM). As a novel structure skeleton natural DHODH inhibitor, **Fr. 1-4** was competent to be a lead compound for future structure modification work.

Computer modeling

General properties analysis of the chemicals

According to the previous experience, compounds should possess certain properties to be accepted as drug. Those properties were formulated by Lipinski in 1997. It is a rule of thumb to evaluate drug likeness, or to determine whether a chemical compound with a certain pharmacological or biological activity has properties that would make it a likely active drug. The properties are summarized as 'Lipinski's rule of five' (28). It is suggested that any pairwise combination of the following conditions: molecular weight >500, log p > 5, hydrogen bond donors >5, hydrogen bond acceptors >10 or rotatable bonds>10 may result in compounds with poor permeability. In this connection, it is very much clear from Table 1 that the purified chemicals comply perfectly with the Lipinski's Rule of Five and are considered to be more likely to have good absorption and permeability.

Docking analysis

Next, we have performed a docking study to understand the interactions between the dihydroorotate dehydrogenase (DHODH) enzyme and its inhibitors to explore their binding mode using the Libdock method of receptor–ligand interactions protocol under DISCOVERY STUDIO 2.5. The inhibitors were found at the coenzyme Q site, as expected. L-dihydroorotate (DHO) and flavin mononucleotide (FMN) were also observed in the structures which were solved at a resolution of 1.9–2.1 Å. Because only compound **Fr. 1-4** had satisfying *in vitro* inhibition capacity, the following docking analysis focused on how the compound **Fr. 1-4** interacting with the protein receptor. The complexes of human DHODH with brequinar (PDB ID 1D3G) and of human DHODH with a teriflunomide (PDB ID 1D3H) were chosen for the docking analysis. The two different human DHODH complexes were selected to ascertain whether differences in the conformation of active site pocket side chains might affect the binding mode, as observed by Baumgartner and co-workers (29).

Leflunomide is an isoxazol derivative, which acts as a prodrug. After absorption, it is rapidly converted into its active metabolite teriflunomide (A771726), which is assigned to the Z-configuration. Brequinar (BQN) was developed for cancer therapy, but failed in clinical trials due to limited therapeutic windows (30). In the complexes 1D3G and 1D3H, the binding sites for both A771726 and Brequinar are located at the narrow end of the channel that ubiquinone uses to accomplish a redox reaction with FMN. Several charged and polar side chains (Gln47, His56, Tyr356, Thr360, and Arg136) are present at this position. In the case of A771726, the deprotonated enolic hydroxy group interacts via hydrogen bond with Tyr356, while the amide carbonyl is hydrogen bonded to Arg136 through a water molecule (Figure 2A). Moving to BQN, the binding mode is quite different. Here, the carboxylate group forms a salt bridge with Arg136 and is hydrogen bonded to Gln47. In addition, the biphenyl moiety establishes a number of hydrophobic contacts with several lipophilic residues of the tunnel (Figure 2).

The docking protocol is able to accurately reproduce the brequinar and teriflunomide experimental pose in 1D3G and 1D3H (Figure 2), which means the docking results of the docking are credible. Moving to **Fr. 1-4**, wide differences are observed between the poses obtained on 1D3G and 1D3H. The results of the docking work with 1D3G and **Fr. 1-4** as receptor and ligands show that **Fr. 1-4** cannot insert into the activity channel to interact

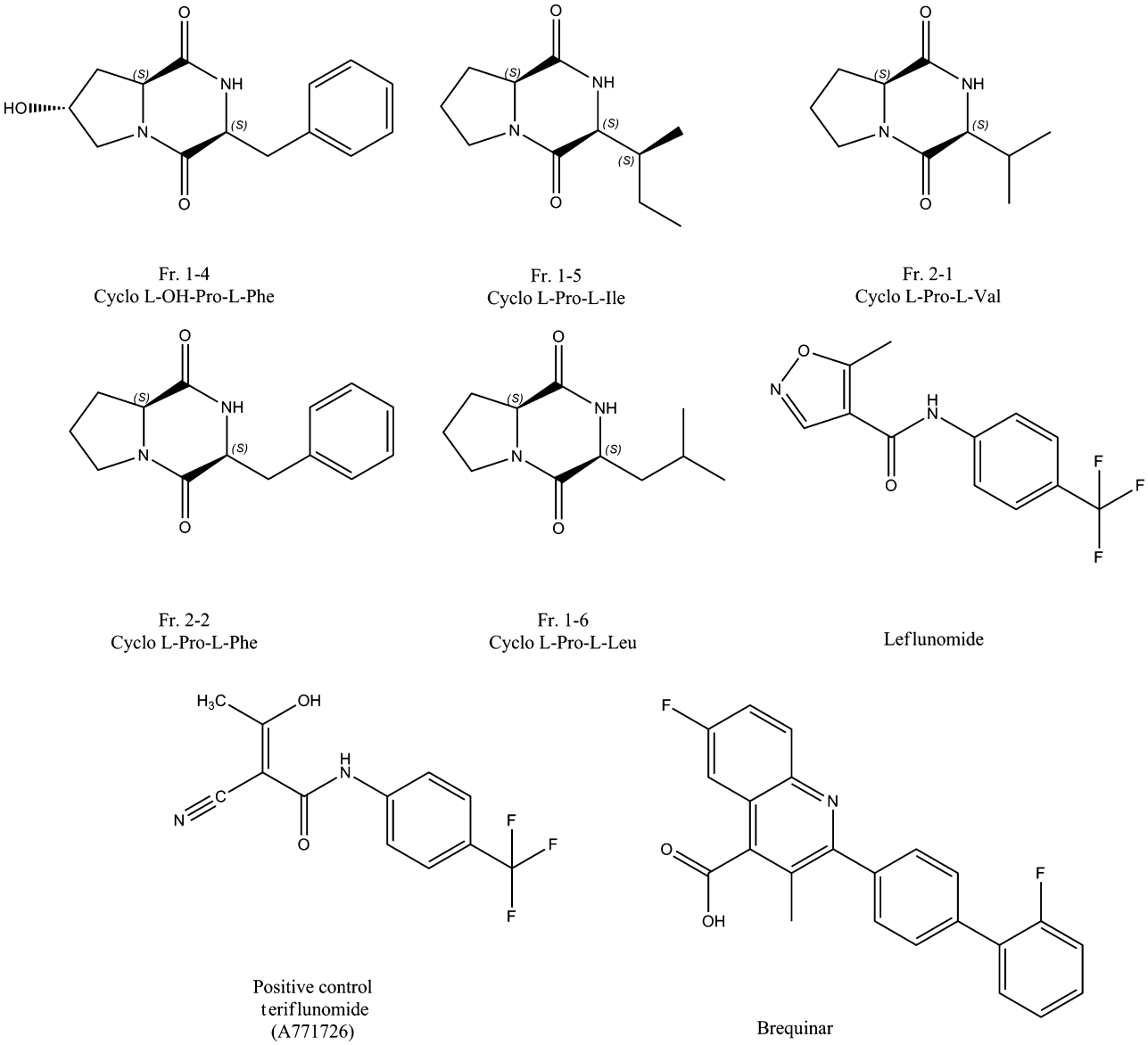

Figure 1: Structures of the purified compounds.

Table 1: Dihydroorotate dehydrogenase inhibition capacity, Libdock scores, and general properties of cyclo dipeptides

		Libdock score						
Chemicals	IC50 ± SE (μM)	1D3H	1D3G	Log p	Molecular weight	Hbond acceptors	Hbond donors	Rotatable bonds
Fr. 1-4	0.773 ± 0.007	107.51	68.34	−0.129	260.288	3	2	2
Fr. 1-5	≥50	94.53	59.65	0.705	210.273	2	1	2
Fr. 1-6	≥50	86.44	61.81	0.637	210.273	2	1	2
Fr. 2-2	≥50	92.433	69.75	0.962	244.289	2	1	2
Fr. 2-1	≥50	86.123	56.88	0.249	196.246	2	1	1
Teriflunomide	0.064 ± 0.004	105.86		2.091	270.207	3	2	3
Brequinar			132.80	4.534	374.36	3	1	3

with any charged and polar side chains (Gln47, His56, Tyr356, Thr360, and Arg136) (Figure 4D). So no hydrogen bond is observed in 1D3G-**Fr. 1-4** docking results. On the contrary, **Fr. 1-4** can easily contact the polar pocket at the end of the activity channel of 1D3H (Figure 4A). Several hydrogen bonds are formed between **Fr. 1-4** and the receptor 1D3H. All the cases indicated that **Fr. 1-4** can only bind with 1D3H and the binding

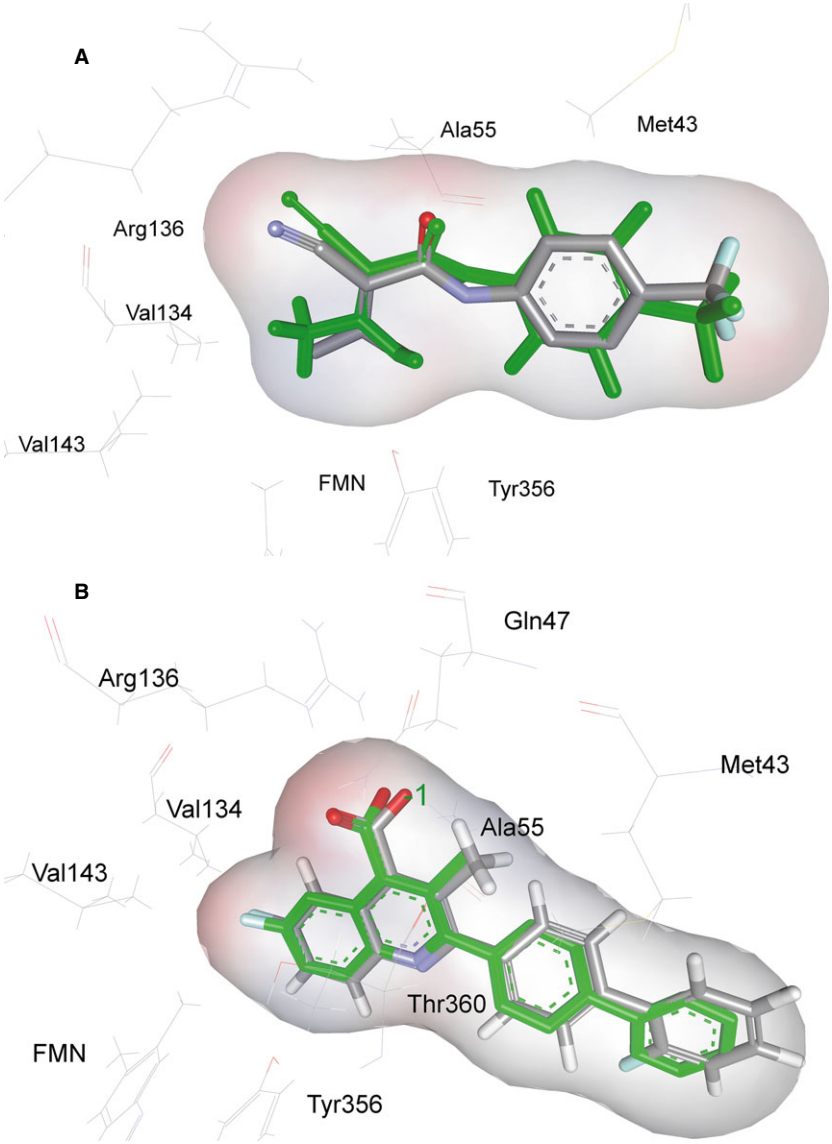

Figure 2: Experimental (colored by elements) and *in silico* docking (colored in green) results of positive control teriflunomide interacting with 1D3H (A) and brequinar with 1D3G (B). Green dotted line indicates hydrogen bond formation.

pose is in a teriflunomide-like fashion. The binding modes of **Fr. 1-4** and positive controls are shown in Figures 3 and 4.

For compound **Fr. 1-4** (shown in Figures 3A and 4A), a hydrogen bond network is observed around the hydroxyl group at the Pro-γ-carbon site, which not only makes hydrogen bonds to a water molecular (H201) but also to Arg136. We speculate that these Hbonds provide main electrostatic interaction power, and it is also the primary reason why **Fr. 1-4** has some activity. However, compared with positive control A771726, the Hbond power of **Fr. 1-4** is much weaker. As it is shown in Figure 3C, A771726 not only can form Hbond with Arg136 through a water molecular, but also can construct Hbond interaction with Tyr356. We think it is part of the reason why the activity of **Fr. 1-4** is weaker than that of A771726. Comparing the binding mode of **Fr. 1-4** with that of **Fr. 2-2**, we can obtain more information about how important the hydroxyl group to **Fr. 1-4** to make it active. As it is demonstrated in Figure 3B, without the hydroxyl group, **Fr. 2-2** cannot form any Hbond with protein receptor in the same docking parameters settings. **Fr. 2-2** only rely on the weak Electrostatic and Van der Waals interactions to dock with protein receptor. We think it is the part of the reason why **Fr. 2-2** do not have activity.

Decomposition of the binding free energy

To gain a detailed picture of the inhibitor/DHODH interactions, the binding free energy was decomposed into inhibitor–residue pairs. The quantitative information is extremely useful to understand the difference of the binding mechanism between **Fr. 1-4** and **Fr. 2-2**. The Electrostatic and Van der Waals interactions between the inhibitors and the important residues of DHODH can be observed in Figure 4.

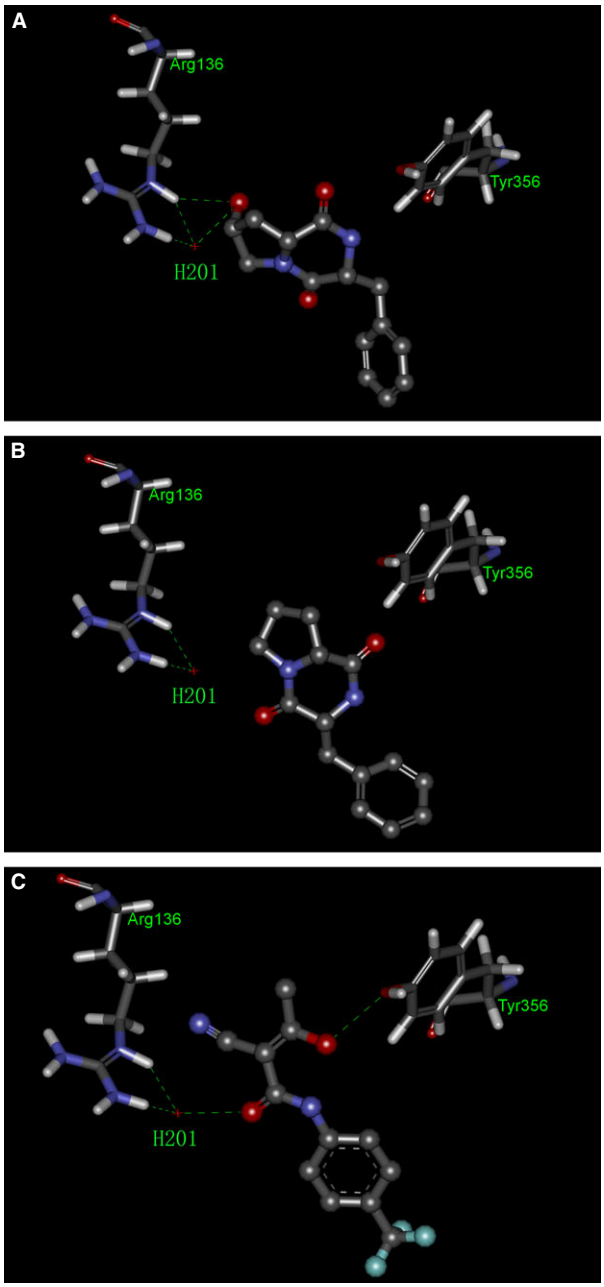

Figure 3: The interaction mode of **Fr. 1-4** (A), **Fr. 2-2** (B), and positive control teriflunomide (C) with Arg136 and Tyr 356.

From Figure 4, one can see that the inhibitors **Fr. 1-4** and **Fr. 2-2** share the similar binding mode. Comparison of energy between **Fr. 1-4** and **Fr. 2-2** shows that interactions of **Fr. 1-4** with Met43, Asp51, Glu53, and Thr360 (−0.9, −1.373, −0.939, and −0.709 kcal/mol) are stronger than those of **Fr. 2-2** (−0.524, −0.806, −0.811, and 0.451 kcal/mol) (Tables S1 and S2). However, the interactions of **Fr. 2-2** with Tyr356 and Leu359 (−0.303 and −0.791 kcal/mol) are stronger than those of **Fr. 1-4** (0.238 and −0.092 kcal/mol). It is demonstrated in the Figure 4 that most of the interaction residues provide van der Waals energy. So the differences of the van der Waals power may be the main reason leading to the large biological activities differences. To prove our inference, we compared the van der Waals energy interaction between inhibitors and the important residues. As it is shown in Tables S1 and S2, the interactions of **Fr. 1-4** with Gln47, Pro52, Arg136, Tyr356, Leu359, and Thr 360 (−0.831, −1.012, −0.657, −1.283, −2.31, and −3.439 kcal/mol) are much stronger than those of **Fr. 2-2** (−0.224, −0.538, −0.298, −0.721, −1.878, and −2.603 kcal/mol). Only one residue Phe62 (−0.132 kcal/mol) interacting with **Fr. 1-4** has lower van der Waals interaction energy than that of **Fr. 2-2**. The result is consistent with the inhibitor activity result in Table 1, which supports our inference that the difference of the van der Waals interactions between ligand and protein determine the difference of the activities between **Fr. 1-4** and **Fr. 2-2**.

The electrostatic interaction of **Fr. 1-4** with Arg136 (−3.234 kcal/mol) is much stronger than any other residues. This phenomenon is the result from the hydrogen bonds between **Fr. 1-4** hydroxyl group and Arg136 mentioned above. It is expected that this hydrogen bond electrostatic interaction energy of **Fr. 1-4** with Arg136 is much stronger than that of **Fr. 2-2**, but unexpectedly the total electrostatic energy (G_{ele}) of **Fr. 1-4** is generally the same as that of **Fr. 2-2**. Comparison of the total van der Waals energy (G_{vdw}), electrostatic energy (G_{ele}), and solvation free energy ($G_{solvation}$) of **Fr. 1-4** (−18.368, −3.417 and 17.118 kcal/mol) and **Fr. 2-2** (−14.731, −4.012 and 18.543 kcal/mol) complex shows that the main promotion energy for interaction is van der waals energy and the main opposition energy is solvation free energy. Although electrostatic interactions are generally the same in both of the complexes, the total van der Waals energy of **Fr. 1-4** is much stronger than that of **Fr. 2-2**. We think the Hbond of **Fr. 1-4** can improve the binding mode of the inhibitor in the pocket. With the assistance of Hbond, inhibitor can obtain more van der Waals from the non-polar residues. From the results we obtain above, we get the conclusion that the hydrogen bond is very important for the binding of **Fr. 1-4**. This Hbond of **Fr. 1-4** cannot contribute much electrostatic energy to the complex but can help the inhibitor to maintain the right binding mode to gain more van der Waals energy from the non-polar residues.

Chemical structure–biological effect relationship analysis

It can be clearly demonstrated from Figure 5 that the active pocket of DHODH is like an asymmetric sandwich. In the middle of the sandwich, a polar residue ring constructed of Gln47, Arg136, and Tyr 356 is observed. These polar residues can form electrostatic interactions with the ligands, which help ligands to dock with protein better by making them closer to the protein receptor to gain more van der Waals energy. The diketopiperazine structure has two Hbond donors and two Hbond

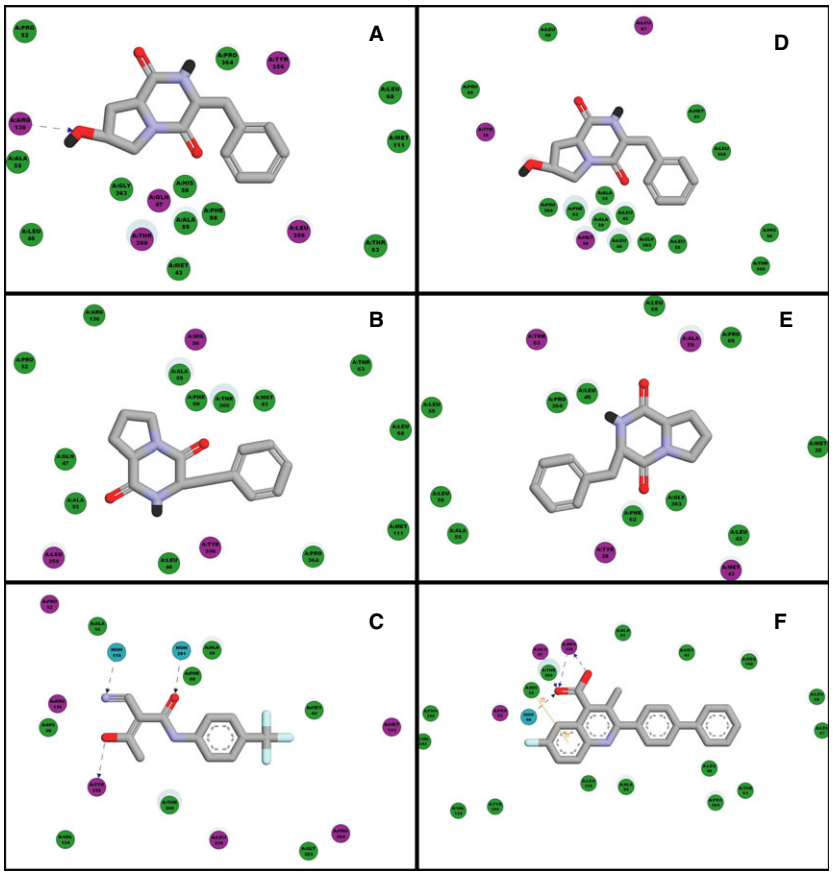

Figure 4: The interaction of **Fr. 1-4** (A), **Fr. 2-2** (B), and positive control teriflunomide (C) with 1D3H and the interaction of **Fr. 1-4** (D), **Fr. 2-2** (E), and positive control teriflunomide (F) with 1D3G. The purple bubbles are the residues mainly providing electrostatic binding energy, and the green bubbles are the residues mainly providing van der Waals binding energy.

acceptors and so, this structure can easily interact with polar residues to help obtaining van der Waals power. This diketopiperazine structure can serve as the core structure for the future DHODH chemical derivation design. The head (Val143 and Val134) and the tail (Ala55, Leu359, Ala59, Met43, Leu46, Pro364, Leu68, and Leu67) of the pocket are full of non-polar residues which mainly provide van der Waals energy. It is suggested that chemicals with higher Log p will interact with these residues better. Compared with positive

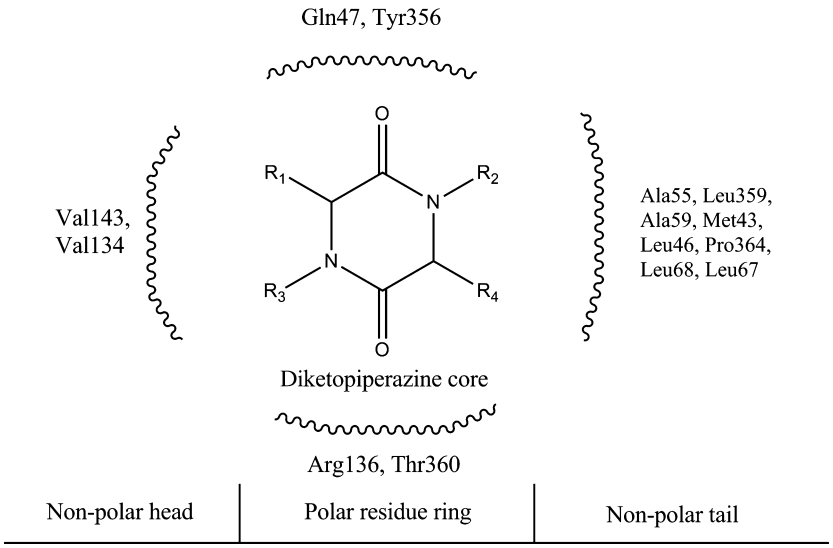

Figure 5: The binding mode analysis of diketopiperazine chemicals in DHODH active pocket.

controls, the Log p of the dipeptides are too low. So in the future chemical modification work, adding some hydrophobic groups at the sides of the diketopiperazine core will make the new derivatives more suitable for binding in the active pocket of DHODH to show lower IC_{50} value.

Conclusions

A practical 2D-preparation method was employed for the purification of high-purity compounds from the Osteon Myospalacem Baileyi extract. A DAISO C18 prep column was used to make fractions in the first dimensional preparation. Then, an YMC C18 AQ column was used to prepare compounds of high purity in the second dimensional preparation. Benefiting from good orthogonality and optimized collection operation, nine compounds (**Fr. 1-4**, 14.1 mg), (**Fr. 1-5**, 12.8 mg), (**Fr. 1-6**, 12.6 mg), (**Fr. 2-1**, 22.1 mg), and (**Fr. 2-2**, 19.2 mg) with more than 98% purity were yielded in the second dimensional preparation. The docking study compared the poses of active DHODH inhibitor **Fr. 1-4**, non-active chemical **Fr. 2-2**, and positive control teriflunomide. The Hbond interaction of hydroxyl group at the Pro-γ-carbon site with Arg136 was the reason why **Fr. 1-4** has inhibition activity but **Fr. 2-2** do not. Chemical **Fr. 1-4** and positive control teriflunomide had almost the same binding mode at the Arg136 site, but **Fr. 1-4** could not form Hbonds with Tyr356. It was part of the reasons why IC_{50} of **Fr. 1-4** was higher than that of teriflunomide. From energy decomposition analysis, it was found that the Hbond could not provide much electrostatic energy to total binding energy but could help the ligands to gain more van der Waals energy by correcting their binding poses. At last, we suggested diketopiperazine structure could serve as the core structure for the future modification work due to its good affinity to the polar residue ring in the middle of the binding pocket. However, the natural diketopiperazine chemicals had too low Log p value. It was suggested that adding some hydrophobic groups at the sides of the diketopiperazine core could help new ligands to bind in the active pocket better.

Acknowledgments

This work was supported by Qinghai Province Natural Science Foundation (2012-Z-901) and National Natural Science Foundation of China (21202196).

References

1. Zhao X.H., Jiang F.Q., Yue H.L., Shao Y., Tao Y.D. (2007) The pharmacodynamics study of Osteon Myospalacem Baileyi extract on experimental rheumatoid arthritis rat model. Chinese Tradit Patent Med;29:1221–1223.
2. Hai P. (2002) Study on Osteon Myospalacem Baileyi bone in treating osteoporotic rats. Shandong J Tradit Chin Med;21:231–233.
3. Hai P. (2001) The analgesic activity of Osteon Myospalacem Baileyi and its effect on single amine neurotransmitter in the brain. Shandong J Tradit Chin Med;20:232–235.
4. Hai P. (2000) The anti-inflammatory effects of Osteon Myospalacem Baileyi extract. Liaoning J Tradit Chin Med;27:524–526.
5. Vollmer M., Horth P., Nagele E. (2004) Optimization of two-dimensional off-line LC/MS separations to improve resolution of complex proteomic samples. Anal Chem;76:5180–5185.
6. Moon P.G., Kwack M.H., Lee J.E., Cho Y.E., Park J.H., Huang D., Moon K.K., Kim J.C., Sung Y.K., Back M.C. (2013) Proteomic analysis of balding and non-balding mesenchyme-derived dermal papilla cells from androgenetic alopecia patients using on-line two-dimensional reversed phase-reversed phase LC-MS/MS. J Proteomics;85:174–191.
7. Gray M.J., Dennis G.R., Slonecker P.J., Shalliker R.A. (2004) Comprehensive two-dimensional separations of complex mixtures using reversed-phase reversed-phase liquid chromatography. J Chromatogra A;1041:101–110.
8. Gray M.J., Dennis G.R., Slonecker P.J., Shalliker R.A. (2003) Evaluation of the two-dimensional reversed-phase–reversed-phase separations of low-molecular mass polystyrenes. J Chromatogra A;1015:89–98.
9. Gray M., Dennis G.R., Wormell P., Shalliker R.A., Slonecker P. (2002) Two dimensional reversed-phase–reversed-phase separations Isomeric separations incorporating C_{18} and carbon clad zirconia stationary phases. J Chromatogra A;975:285–297.
10. Jia J.M., Ma X.C., Wu C.F., Hu G.S. (2005) Cordycedipeptide A, a new cyclodipeptide from the culture liquid of *cordyceps sinensis* (BERK.) Sacc. Chem Pharm Bull;53:582–583.
11. Stark T., Hoffmann T. (2005) Structures, sensory activity, and dose/response functions of 2, 5-diketopiperazines in roasted cocoa nibs (Theobroma cacao). J Agr Food Chem;53:7222–7231.
12. Ginz M., Engelhardt U.H. (2000) Identification of proline-based diketopiperazines in roasted coffee. J Agr Food Chem;48:3528–3532.
13. Vergne C., Esnault N.B., Perez T., Martin M.T., Adeline M.T., Dau E.T.H., Mourabit A.A. (2006) Verpacamides A-D, a sequence of C11N5 diketopiperazines relating cyclo (Pro-Pro) to cyclo (Pro-Arg), from the marine sponge axinella vaceleti: possible biogenetic precursors of pyrrole-2-aminoimidazole alkaloids. Org Lett;8:2421–2424.
14. Fischer P.M. (2003) Diketopiperazines in peptide and combinatorial chemistry. J Pept Sci;9:9–35.
15. Horton D.A., Bourne G.T., Smythe M.L. (2000) Exploring privileged structures: the combinatorial synthesis of cyclic peptides. Mol Divers;5:289–304.

16. Wang D.X., Liang M.T., Tian G.J., Lin H., Liu H.Q. (2002) A facile pathway to synthesize diketopiperazine derivatives. Tetrahedron Lett;43:865–867.
17. Evans D.R., Guy H.I. (2004) Mammalian pyrimidine biosynthesis: fresh insights into an ancient pathway. J Biol Chem;279:33035–33038.
18. Baldwin J., Michnoff C.H., Malmquist N.A., White J., Roth M.G., Rathod P.K., Phillips M.A. (2005) High-throughput screening for potent and selective inhibitors of plasmodium falciparum dihydroorotate dehydrogenase. J Biol Chem;280:21847–21853.
19. Bausann P., Mandl-Weber S., Volkl A., Adam C., Bumeder I., Oduncu F., Schmidmaier R. (2009) Dihydroorotate dehydrogenase inhibitor A771726 (leflunomide) induces apoptosis and diminishes proliferation of multiple myeloma cells. Mol Cancer Ther;8:366–375.
20. Chen S.F., Ruben R.L., Dexter D.L. (1986) Mechanism of action of the novel anticancer agent 6-Fluoro-2-(2′-fluoro-1, 1′-biphenyl-4-yl)-3-methyl-4-quinolinecarboxylic acid sodium salt (NSC 368390): inhibition of de novo pyrimidine nucleotide biosynthesis. Cancer Res;46:5014–5019.
21. Herrmann M.L., Schleyerbach R., Kirschbaum B. (2000) Leflunomide: an immunomodulatory drug for the treatment of rheumatoid arthritis and other autoimmune diseases. Immunopharm;47:273–289.
22. Merrill J.E., Hanak S., Pu S.F., Liang J., Dang C., Iglesias-Bregna D., Harvey B., Zhu B., McMonagle-Strucko K. (2009) Teriflunomide reduces behavioral, electrophysiological, and histopathological deficits in the Dark Agouti rat model of experimental autoimmune encephalomyelitis. J Neurol;256:89–103.
23. Subbayya I.N., Ray S.S., Balaram P., Balaram H. (1997) Metabotic enzymes as potential drug targets in *plasmodium falciparum*. Indian J Med Res;106:79–94.
24. Arakaki T.L., Buckner F.S., Gillespie J.R., Malmquist N.A., Phillips M.A., Kalyuzhniy O., Luft J.R., Detitta G.T., Verlinde C.L., Van Voorhis W.C., Hol W.G., Merritt E.A. (2008) Characterization of *Trypanosoma brucei* dihydroorotate dehydrogenase as a possible drug target; structural, kinetic and RNAi studies. Mol Microbiol;68:37–50.
25. Liu X., Dong G., Zhang J., Qi J., Zheng C., Zhou Y., Zhu J., Sheng C., Lu J. (2011) Discovery of novel human acrosin inhibitors by virtual screening. J Comput Aided Mol Des;25:977–985.
26. Lu C., Zhou L., Li Z., Gao X., Zhang W. (2012) Pharmacophore modeling, virtual screening, and molecular docking studies for discovery of novel Carbonic anhydrase IX inhibitors. Med Chem Res;21:3417–3427.
27. Zhang W., Zhou L., Li Z. (2013) 3D QSAR pharmacophore-based virtual screening and molecular docking studies for the discovery of potential PDK1 inhibitors. Med Chem Res;22:3416–3427.
28. Lipinski C., Lombardo F., Dominy B., Feeney P. (1997) Experimental and computational approaches to estimate solubility and permeability in drug discovery and development settings. Adv Drug Delivery Rev;23:3–25.
29. Baumgartner R., Walloschek M., Kralik M., Gotschlich A., Tasler S., Mies J., Leban J. (2006) Dual binding mode of a novel series of DHODH Inhibitors. J Med Chem;49:1239–1247.
30. Maroun J., Ruckdeschel J., Natale R., Morgan R., Dallaire B., Sisk R., Gyves J. (1993) Multicenter phase II study of brequinar sodium in patients with advanced lung cancer. Cancer Chemoth Pharm;32:64–66.

Supporting Information

Additional Supporting Information may be found in the online version of this article:

Figure S1. First dimensional preparation of crude sample on C18 prep column (50 × 250 mm i.d., 10 μm, 120 Å, DAISO). The elution program was 0–5 min for 18% B, 5–35 min for 18% to 40% B. The flow rate was 80 mL/min. The concentration of the loading sample was 200 mg/mL. The injection volume was 4 mL. Chromatograph was recorded at 214 nm.

Figure S2. HPLC analysis of **Fr. 1** and **2** on YMC C18 AQ column (4.6 × 250 mm i.d., 10 μm, 100 Å, YMC). Isocratic elution procedure for **Fr. 1** was 15% B for 45 min and for **Fr. 2** was 23% B for 27 min. The flow rate was 1 mL/min. The injection volume was 10 μL. Chromatography data were collected at 214 nm.

Figure S3. Second dimensional preparation of **Fr. 1** and **2** on YMC C18 AQ (10 × 250 mm i.d., 10 μm, 100 Å) column. Isocratic elution procedure for **Fr. 1** was 15% for 40 min and for **Fr. 2** was 23% B for 30 min. The sample concentration was 500 mg/mL. The injection volume was 700 μL. The flow rate was 4 mL/min. Chromatography data were collected at 214 nm.

Figure S4. Purity evaluations of single compounds on YMC C18 AQ column (4.6 × 250 mm, 5 μm, 100 Å, YMC). The flow rate was 1 mL/min. The injection volume was 10 μL. The linear gradient elution procedure for **Fr. 1-4**, **Fr. 1-5**, and **Fr. 1-6** was 10% to 25% B for 30 min, for **Fr. 2-1** and **Fr. 2-2** was 20% to 35% B for 30 min, respectively. Chromatography data were collected at 214 nm.

Table S1. Decomposition analysis of free energy of **Fr. 2-2** (Energy unit is kcal/mol)

Table S2. Decomposition analysis of free energy of **Fr. 1-4** (Energy unit is kcal/mol)

Appendix S1. The optical rotation, nuclear magnetic resonance and mass spectrum data of the purified compounds.